Supplementary Information

Unconventional Charge Compensation Mechanism for Proton Insertion in Aqueous Zn-Ion Batteries

Jiwei Wang,[a] Heran Huang,[b] Linna Qiao,[b] Haonan Wang,[b] Krystal Lee,[a] Guangwen Zhou,[b,c] Hao Liu[a,b]*

[a]Department of Chemistry, Binghamton University, Binghamton, New York 13902, United States

[b] Materials Science and Engineering, Binghamton University, Binghamton, New York 13902, United States

[c] Department of Mechanical Engineering, Binghamton University, Binghamton, New York 13902, United States

Figures S1-S10

Tables S1-S2

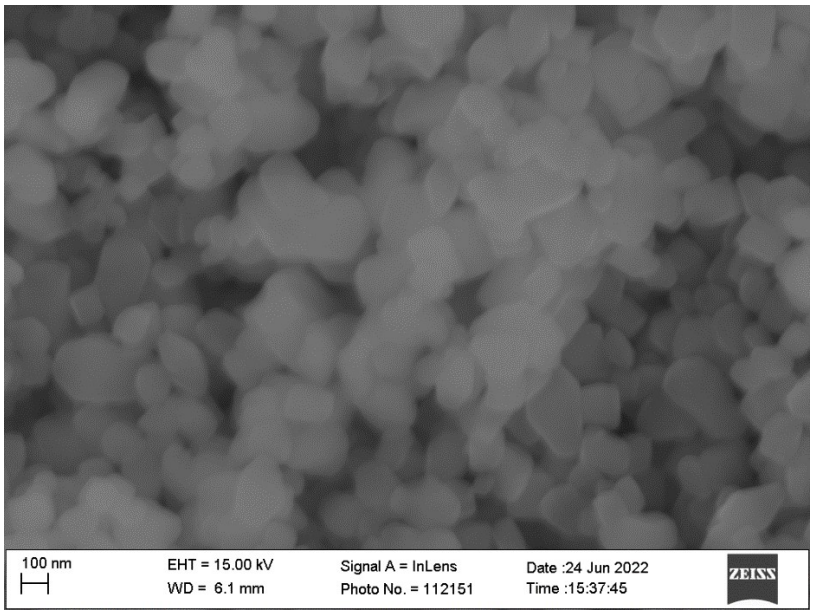

Figure S1. Scanning electron microscopy image of the as-synthesized ε-$VOPO_4$ powder.

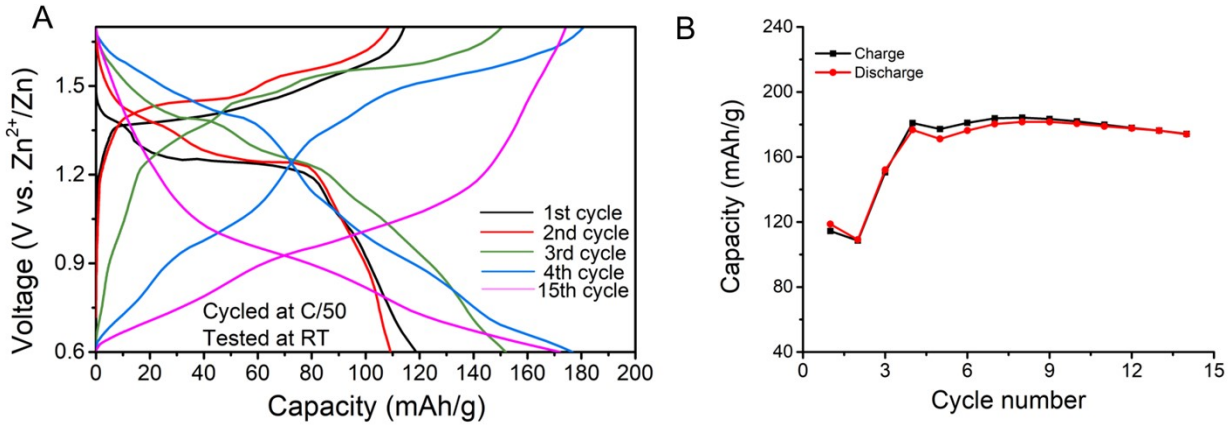

Figure S2. Voltage profile of the galvanostatic cycling of the ε-$VOPO_4$ cathode cycled at C/50 between 0.6 V and 1.7V at different cycles, and (B) the corresponding capacity retention vs cycle number.

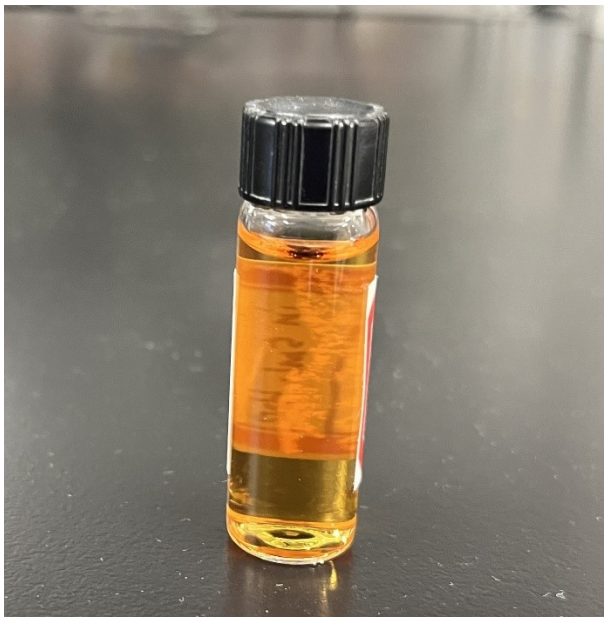

Figure S3. Aqueous solution obtained after soaking the as-synthesized ε-$VOPO_4$ powder in water (1 mg/mL) for 5 days. The ε-$VOPO_4$ powder was completely dissolved in water forming a transparent light orange solution.

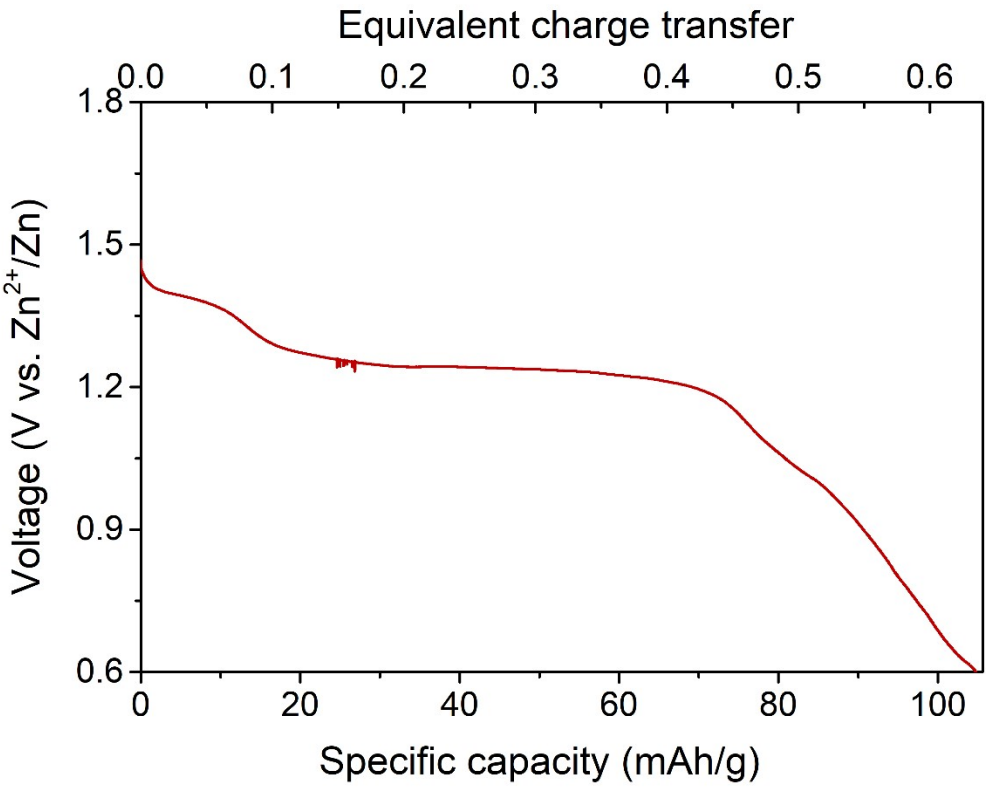

Figure S4. Voltage profile for the discharge of the electrode prepared for the high-resolution XRD.

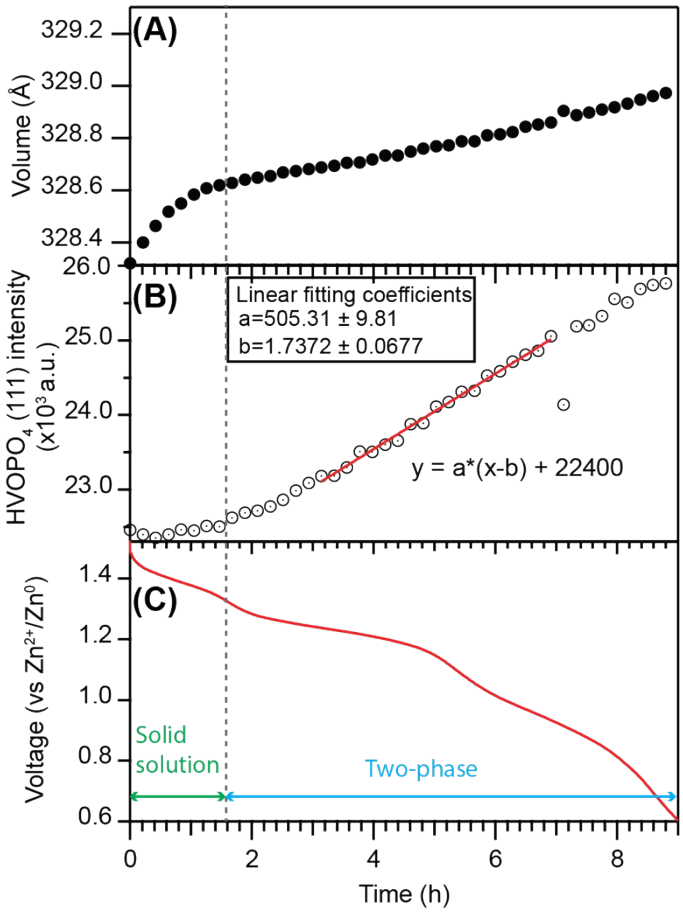

Figure S5. (A) Unit cell volume of $VOPO_4$, (B) intensity of the $HVOPO_4$ (111) peak at 4.2° 2θ, which overlaps with the (200) and (002) peaks of $HVOPO_4$, and (C) discharge voltage profile during the operando XRD measurement.

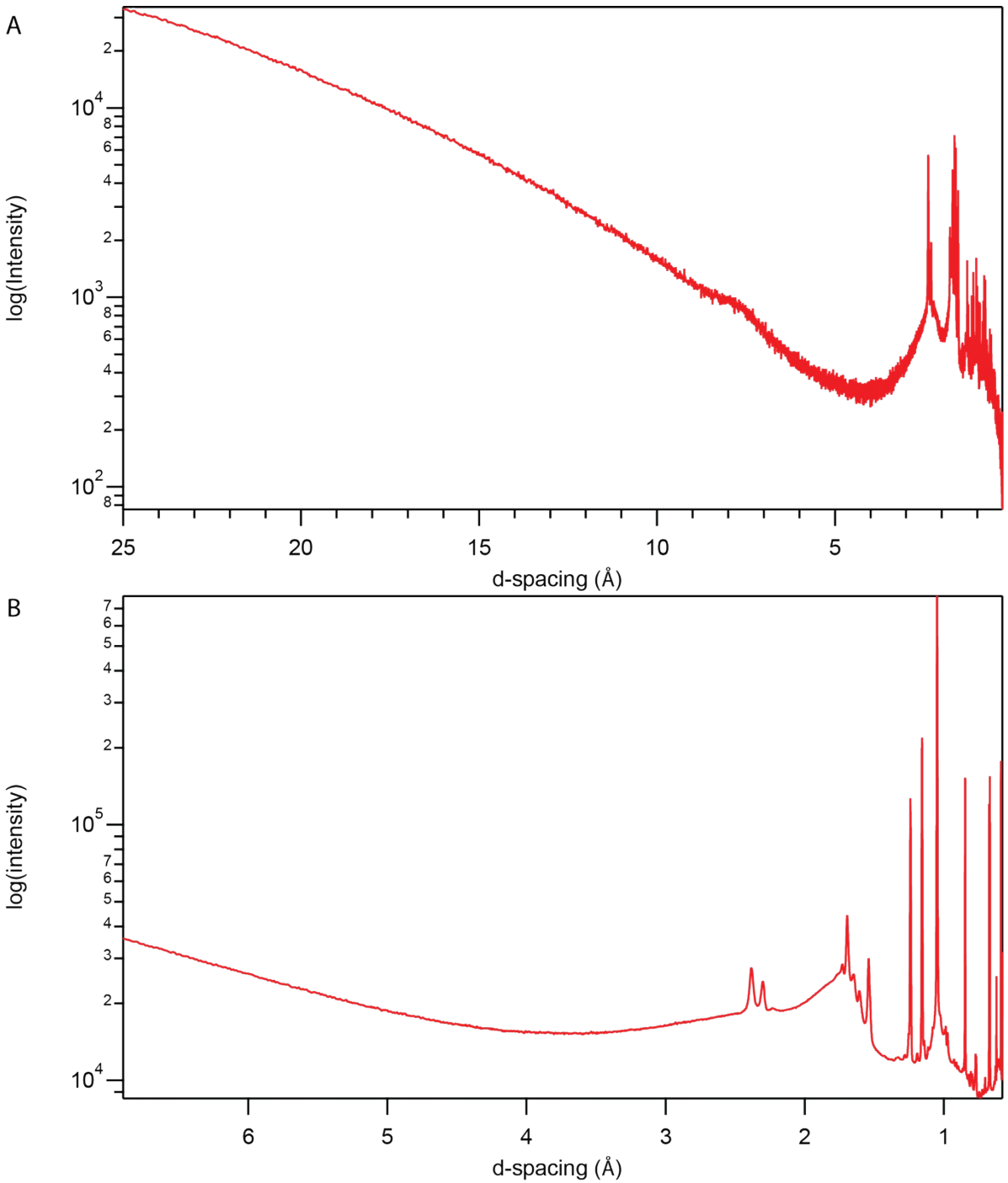

Figure S6. (A) High-resolution synchrotron XRD observed for the $VOPO_4$ electrode discharged to 0.6 V. (B) *Operando* synchrotron XRD observed at the end of discharge at 0.6 V. No peaks are observed above the d-spacing for the first Bragg peak from the $(H)VOPO_4$ phase. The intensity is plotted in logarithmic scale to highlight low intensity features.

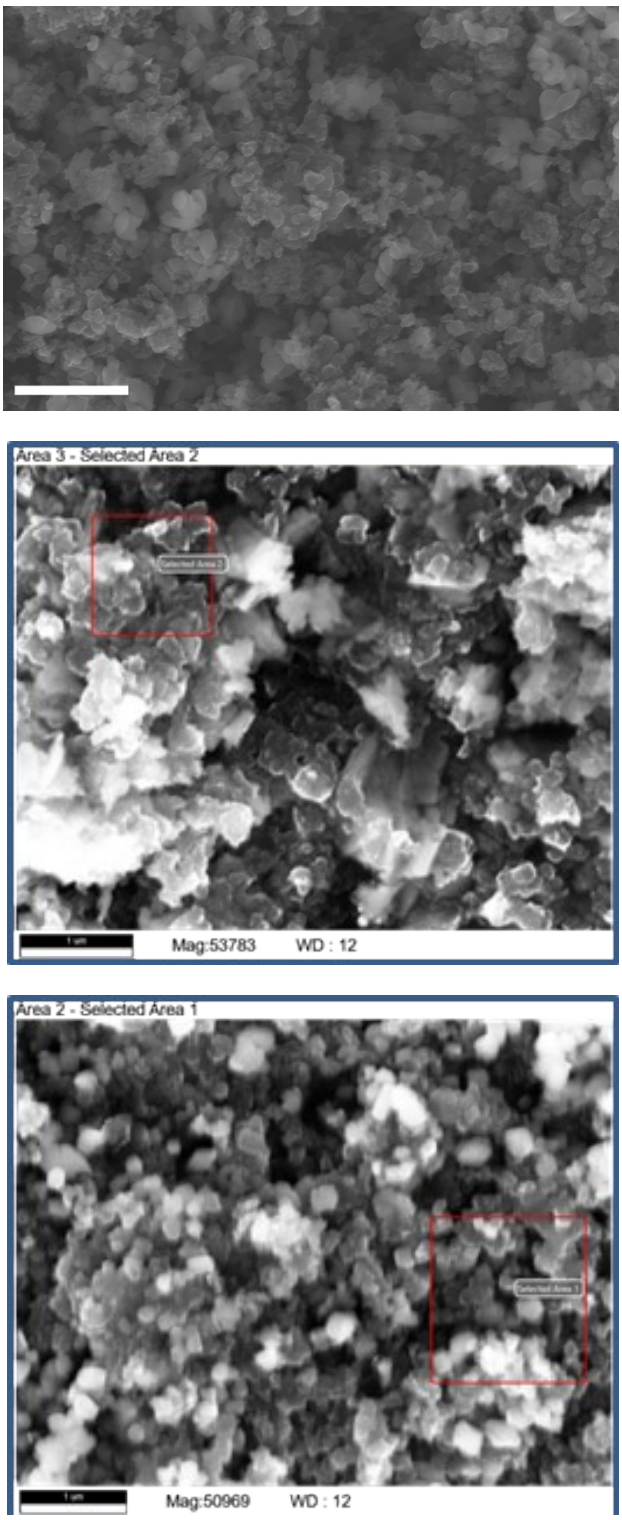

Figure S7. SEM images of the pristine electrode (top) and electrode discharged to 0.6 V (middle) and recharged to 1.7 V (bottom). No significant morphological differences are observed. Scale bar corresponds to 1 μm.

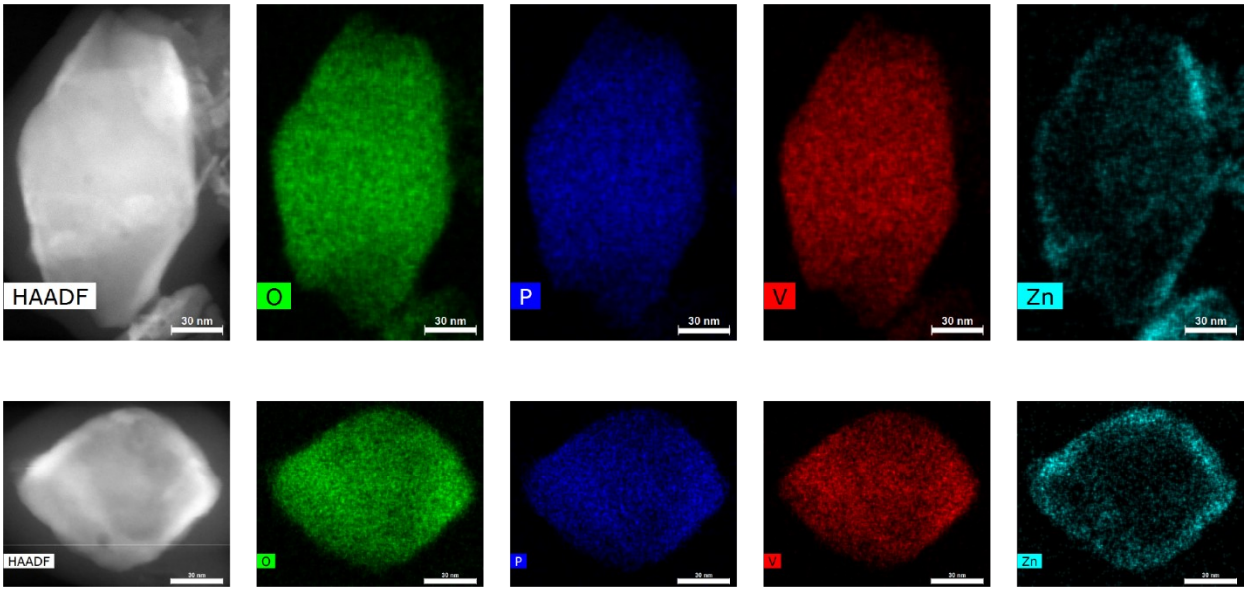

Figure S8. TEM EDS mapping of two particles in the electrode discharged to 0.6 V. Zn primarily accumulates on the particle surface. Scale bar corresponds to 30 nm.

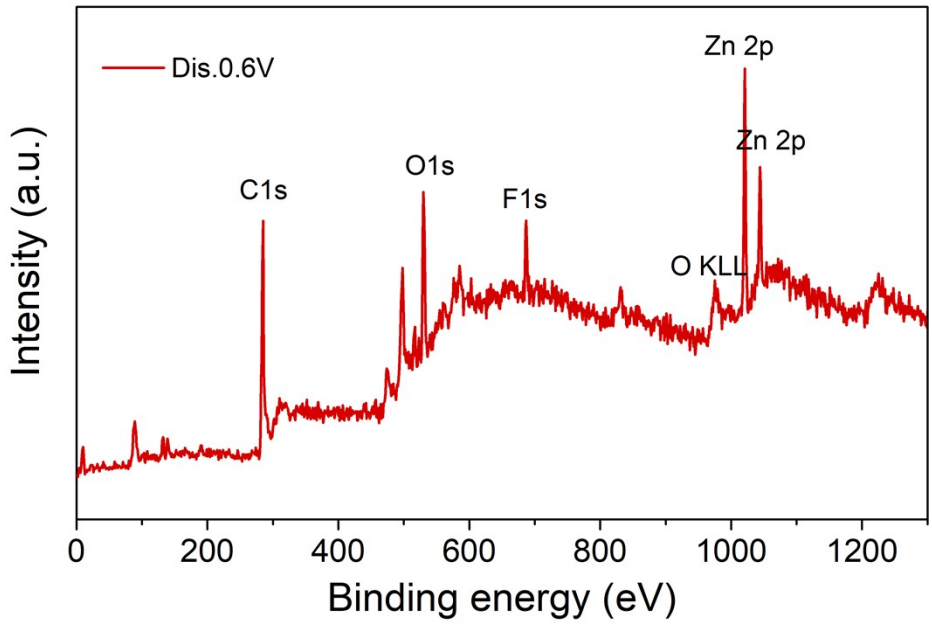

Figure S9. XPS survey spectrum of the electrode discharged to 0.6V.

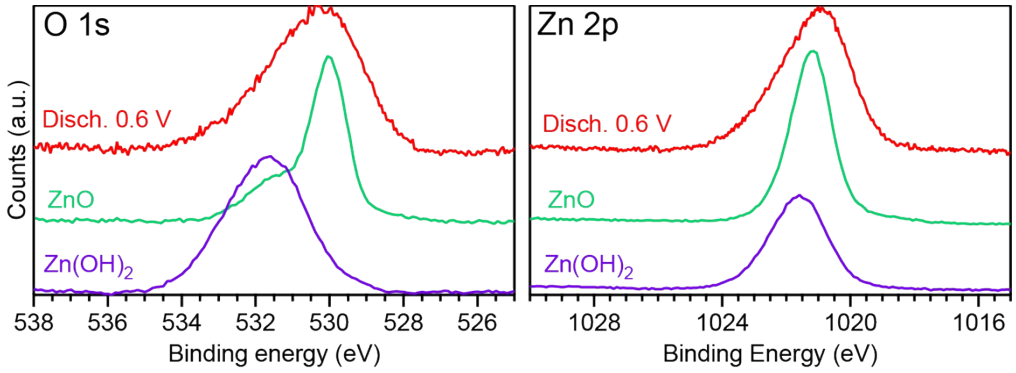

Figure S10. XPS of the O 1s and Zn 2p core levels for ZnO, $Zn(OH)_2$, and the electrode discharged to 0.6 V (Disch. 0.6 V).

Table S1. Refined structure parameters of $HVOPO_4$

a = 7.43003(16) Å, *b* = 7.06750(13) Å, *c* = 7.37430(14) Å, $\alpha = \gamma = 90$ °, $\beta = 120.0659(7)$ °

Volume = 335.135(12) $Å^3$

Site label	atom	x	y	z	occupancy	B	Wyckoff
V1	V	0.4799(5)	0.2579(6)	0.4771(4)	1	2.66(4)	4a
P1	P	0.2176(7)	0.6262(3)	0.2005(6)	1	1	4a
O1	O	0.6944(10)	0.3354(5)	0.6993(13)	1	1	4a
O2	O	0.0290(8)	0.5102(8)	0.0421(8)	1	1	4a
O3	O	0.3806(8)	0.5168(9)	0.4158(10)	1	1	4a
O4	O	0.1193(8)	0.7786(8)	0.2942(7)	1	1	4a
O5	O	0.3199(9)	0.7415(10)	0.1063(8)	1	1	4a

Table S2. Zn 2p3/2 binding energy (BE) reported for cycled electrodes in AZIBs.

BE (eV)	Assignment	Reference
1022.4	$Zn_4(SO_4)(OH)_6 \cdot 5H_2O$	Chem. Mater. 2021, 33, 4089−4098
1022.6	Intercalated Zn in V_2O_5 crystal lattice	Adv. Funct. Mater. 2023, 33, 2303763
1022	$Zn_3(OH)_2V_2O_7 \cdot 3H_2O$	ACS Energy Lett. 2020, 5, 2979−2986
1024 1022	$Zn_{12}(CF_3SO_3)_9(OH)_{15} \cdot xH_2O$	
1022.1	Indigenous Zn in $Zn_{0.25}V_2O_5 \cdot nH_2O$	Nat Commun 14, 3067 (2023).
1023.7 1027.4	Intercalated Zn in $Zn_{0.25}V_2O_5 \cdot nH_2O$	